

Hierarchically Structured Snowflake-like $\text{WO}_3 \cdot 0.33\text{H}_2\text{O}$ Particles Prepared by a Facile, Green, and Microwave-assisted Method

Jiayin Li,^{1,2} Jianfeng Huang,^{*1} Chenglong Yu,¹ Jianpeng Wu,¹ Liyun Cao,¹ and Kazumichi Yanagisawa²

¹Key Laboratory of Auxiliary Chemistry and Technology for Light Chemical Industry,

Ministry of Education, Shaanxi University of Science and Technology, Xi'an 710021, P. R. China

²Research Laboratory of Hydrothermal Chemistry, Faculty of Science, Kochi University,
2-5-1 Akebono-cho, Kochi 780-8520

(Received March 10, 2011; CL-110205; E-mail: huangjf@sust.edu.cn)

In this letter, we report a novel hierarchically structured $\text{WO}_3 \cdot 0.33\text{H}_2\text{O}$ "snowflakes" that were successfully synthesized by a template-free and microwave-assisted hydrothermal method for the first time. Combining the characterization results and its crystal structure together reveals the $\text{WO}_3 \cdot 0.33\text{H}_2\text{O}$ particles have an oriented growth along six equivalent (100) directions in (001) plane to form the novel snowflake-like microstructure, which is significantly different from the sample prepared at conventional hydrothermal conditions. Moreover, microwave heating is considered to accelerate the oriented crystal growth along (100) directions.

Hierarchical nanostructured materials with specific sizes and shapes have attracted great interests in various fields over recent decades. Syntheses of hierarchically assembled nanostructures, including nanowires,^{1,2} nanosponges,³ nanorods,^{4,5} and nanosheets,⁶ are believed to be one of the most promising aspects of nanoscience due to their vast potential applications. Thus, a number of methods have been used for the assembly of many low-dimensional nanostructured materials to obtain controlled morphologies, architectures, and sizes, such as ZnO ,⁷ Al_2O_3 ,⁸ CuS ,⁹ Fe_2O_3 ,¹⁰ and WO_3 .¹¹ However, as the difficulties in crystal nucleation and crystallization remain, it is still of great significance to synthesize the 3D architectures from nanobuilding blocks.

Recently, tungsten oxide hydrates ($\text{WO}_3 \cdot n\text{H}_2\text{O}$, $n = 0-2$) are of particular interest in various fields such as supercapacitors,¹² gas sensors,¹³ photocatalysts,¹⁴ electrochromic devices,¹⁵ and solar energy devices.¹⁶ Among these applications, $\text{WO}_3 \cdot n\text{H}_2\text{O}$ crystallites with controlled morphology, especially with hierarchical structures, showed profound significance due to their novel three-dimensional microstructures.¹⁷⁻¹⁹ Nevertheless, "soft" templates or "hard" templates are often necessary to maintain the specific architectures, resulting in problems of contamination in the particles and the economical efficiency of practical applications. Thus, research on the synthesis of tungsten oxide hydrates by template-free methods has made great achievements^{11,17-21} but still have deficiencies in acquiring controlled morphologies, which involves either long reactions times,^{11,19-21} extremely poisonous starting materials,¹⁷ or expensive W sources like WCl_6 ¹⁸ and $\text{W}(\text{CO})_6$.¹⁷ Peroxo-polytungstic acid is a tungsten-based water-soluble precursor, which can be obtained by simply mixing tungsten powder and hydrogen peroxide solutions together. This acid has been found to prepare nanosized tungsten oxide hydrate materials before,²⁰ but few reports of microwave-irradiated synthesis using this acid have been published yet.

Microwave-assisted hydrothermal method has been considered a good approach to synthesize tungsten oxide hydrate particles. Many researchers have reported this method recently,²²⁻²⁴ introducing a facile, clean, and low-cost approach to synthesize tungsten oxide hydrates in liquid phases. However, few of their results exhibit well-defined shapes and uniform morphologies. This could be attributed to the difficulties in controlling the simultaneous growth of the crystal, which is extremely accelerated by the microwave heating.²⁵ Therefore, syntheses of well-shaped $\text{WO}_3 \cdot n\text{H}_2\text{O}$ particles by microwave-assisted hydrothermal method, especially without any additives, is expected to widely facilitate the utilization of tungsten oxide hydrates in various applications. In this paper, we report a template-free and microwave-assisted hydrothermal synthesis of hierarchically structured $\text{WO}_3 \cdot 0.33\text{H}_2\text{O}$ particles with well-defined snowflake-like shapes. Peroxo-polytungstic acid was first used as precursor under microwave-assisted conditions to obtain uniformly shaped tungsten oxide hydrate particles. An explanation of the interesting morphology is given according to the crystal structure and microwave-assisted growth habits of crystalline $\text{WO}_3 \cdot 0.33\text{H}_2\text{O}$.

The $\text{WO}_3 \cdot 0.33\text{H}_2\text{O}$ snowflake-like particles were synthesized by a microwave-assisted hydrothermal reaction using peroxy-polytungstic acid as precursor. In a typical synthesis, finely powdered tungsten (4 g) was slowly added to hydrogen peroxide (20 mL, 30 wt %) in a cold water bath (10 °C) to stabilize the reaction temperature below 40 °C. This produced a clear and colorless peroxy-polytungstic acid solution.

The as-synthesized solution was then diluted with deionized water to obtain a tungsten concentration of 0.127 mol L⁻¹. The diluted solution was then transferred into a Teflon-lined autoclave (100 mL, filling ratio 60%), the autoclave was treated at 180 °C for 60 min under the temperature-controlled mode of a MDS-8 microwave-assisted hydrothermal (MH) system (Shanghai Sineo Microwave Chemistry Technology Co., Ltd. (China)). The operating power was set to 300 W; heating from room temperature to 180 °C took 15 min, and then the temperature was maintained for one hour. Afterward, the as-prepared white precipitates were isolated by centrifugation and washed with absolute ethanol (20 mL) four times. Finally, the white precipitates were dried at 40 °C in a drying cabinet for 1 h.

The sample phase was characterized via X-ray powder diffraction (XRD) on a D/MAX-2200PC X-ray diffractometer (Rigaku, Japan) with $\text{Cu K}\alpha$ radiation ($\lambda = 0.15406$ nm) at a scanning rate of 8° min⁻¹ in the 2θ range from 5 to 70°. The XRD peak intensities were measured by using Jade 5 software to calculate the relative intensity between peaks. A JSM-6700F field-emission scanning electron microscope was used for field

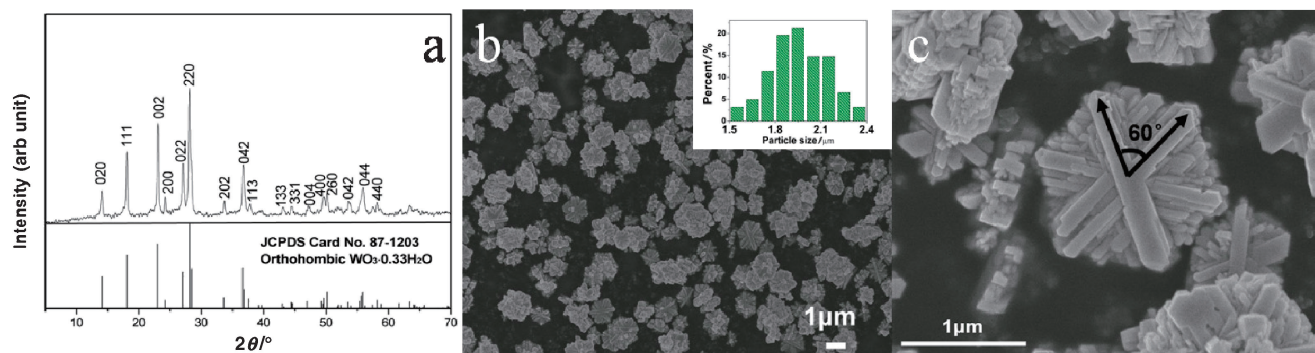


Figure 1. XRD pattern (a) and FESEM images (b, c) of the $\text{WO}_3 \cdot 0.33\text{H}_2\text{O}$ particles by microwave hydrothermal treatment (Inset in Figure 1b is the size distribution of 46 particles in Figure 1b).

emission scanning electron microscopic (FESEM) images. Transmission electron microscopic (TEM) images, high-resolution transmission electron microscopic (HRTEM) images, and selected area electron diffractions (SAED) were taken on a JEM-3010 high-resolution transmission electron microscope operated at 300 kV.

The as-prepared particles are shown by powder XRD pattern (Figure 1a) to consist of the pure orthorhombic $\text{WO}_3 \cdot 0.33\text{H}_2\text{O}$ phase with a space group of $Fmm2$ (Joint Committee on Powder Diffraction Standards, JCPDS Card No. 87-1203). Comparing XRD pattern in JCPDS Card No. 87-1203 to the obtained pattern from the product indicates the relative intensity of the 200 peak to 020 peak increases from 0.26 (JCPDS card) to 0.63 (sample), implying a preferential growth along the $[100]$ direction.

The typical FESEM images of the as-prepared orthorhombic $\text{WO}_3 \cdot 0.33\text{H}_2\text{O}$ powders are shown in Figures 1b and 1c. The low-magnification image in Figure 1b shows that the product consists almost entirely of hexagonal snowflake-like shape with an average size of ca. $1.95 \mu\text{m}$. This indicates the high yield and good uniformity achieved with microwave-assisted approach. The magnified image in Figure 1c shows the morphology of a snowflake growing in six hexasymmetric directions. It presents a clear and well-defined snowflake-like structure with multilayered branches consisting intersection angles of 60° .

Detailed information of this hierarchical structure is shown in Figure 2. The TEM image in Figure 2a shows a typical particle that has a similar hexagonal outline to the particles in FESEM images. It exhibits various shades on the edge of the particle that suggest a multilayer structure with several thin sheets in the “snowflake.” For further structural characterization, the HRTEM image and the related fast Fourier transformation pattern were taken from one of the sheets in Figure 2a, as shown in Figure 2b. They all exhibit clear lattice fringes that suggest the sheet has a single-crystal structure. The interplanar distances of 0.63 nm between adjacent lattice planes are accord with the distance between two (020) crystal planes. The SAED pattern (Figure 2c) taken from Figure 2b shows the $[001]$ zone axis with diffraction spots along the $[010]$ and $[\bar{3}10]$ directions. This reveals that the sheet is exposed with (110), (001), $(1\bar{1}0)$, and (010) faces and that it has a preferential growth along the $[100]$ direction, which corresponds to the XRD results. Furthermore, combining the FESEM and HRTEM results together reveals the multilayered sheets are oriented along $[001]$ with branchlike

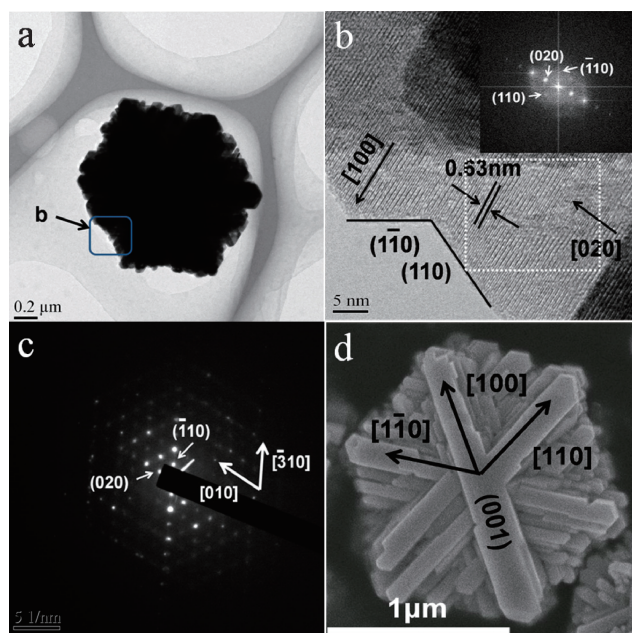


Figure 2. TEM, HRTEM, and SAED results of one hexagonal snowflake-like particle: (a) TEM image of a hexagonal snowflake-like particle, (b) HRTEM image recorded on the marked edge of the particle in Figure 2a (Inset: a calculated FFT pattern from the selected area), (c) SAED pattern of the sheet-like structure in (b), and (d) illustration of the branchlike structures.

structure growing along $[100]$, $[110]$, and $[\bar{1}10]$ directions. Thus, the snowflake-like structures are resulting from the growth along six directions, $\pm[100]$, $\pm[110]$, and $\pm[\bar{1}10]$, to form a hexagonally shaped outline (Figure 2d).

The crystal structure of $\text{WO}_3 \cdot 0.33\text{H}_2\text{O}$ is thought to be a fundamental factor to maintain the snowflake-like microstructure in this research. In the $\text{WO}_3 \cdot 0.33\text{H}_2\text{O}$ crystal structure, $[\text{WO}_6]$ octahedra are connected by corner sharing to form an infinite layer in $\{001\}$ planes. This layer is presented by the graphical representation of the projection along $[001]$ direction in Figure 3a. The projection exhibits three equivalent interplanar distances in the (001) plane in Figure 3b, suggesting a hexasymmetric structure with six equivalent directions of

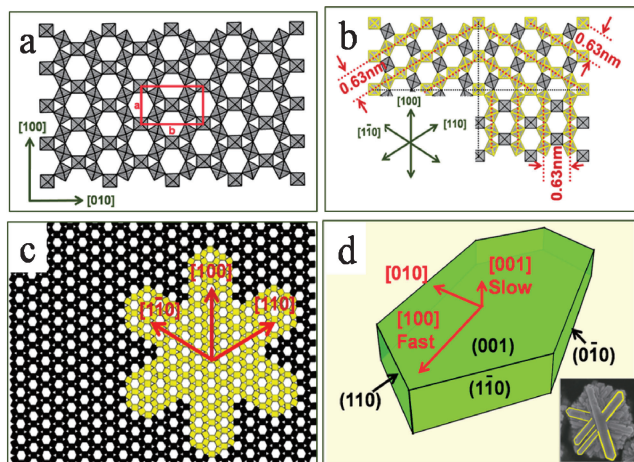


Figure 3. Schematic illustration of the hexasymmetric orthorhombic $\text{WO}_3 \cdot 0.33\text{H}_2\text{O}$ structure viewing along $[001]$ (each small tetragon stands for a $[\text{WO}_6]$ octahedra): (a) Standard layout of the $\text{WO}_3 \cdot 0.33\text{H}_2\text{O}$ structure with a unit cell marked by the rectangle. (b) $\text{WO}_3 \cdot 0.33\text{H}_2\text{O}$ structure with three equivalent interplanar spaces. (c) Schematic view of snowflakelike structure with preferential growth in three directions. (d) The illustration of the $\text{WO}_3 \cdot 0.33\text{H}_2\text{O}$ crystal growth of one nanosheet in the “snowflake” (Inset in Figure 3d: A snowflakelike particle with several edge-marked nanosheets).

$\langle 100 \rangle$ in the (001) plane. If the crystal growth along $\langle 100 \rangle$ directions initiates faster than $\langle 010 \rangle$ and $\langle 001 \rangle$ directions, a hexasymmetric shape would form in the (001) plane, as is shown in Figure 3c. This hexasymmetric structure will grow at various positions when the origin site and initial time of crystal growth differs, which would form hierarchical branching structures along six equivalent $\langle 100 \rangle$ directions.

As for why the growth along six crystallographic $\langle 100 \rangle$ directions is faster than other directions, the discussions of the crystal growth habits and the microwave heating method are necessary. It is well known that under equilibrium conditions, crystal growth along the direction perpendicular to the face with the highest surface energy possesses the fastest growth rate, leading to an elimination of faces with higher surface free energy and exposure of the lower-energy faces.²⁶ In the orthorhombic $\text{WO}_3 \cdot 0.33\text{H}_2\text{O}$ structure, the surface energy of different faces have the order of $\{100\} > \{010\} > \{001\}$.²⁰ This results in the fastest and slowest crystal growth along $[100]$ and $[001]$ direction, respectively, as is shown in Figure 3d. However, note that such morphology was not maintained under the same condition by conventional hydrothermal method.²⁰ Therefore, microwave heating is believed to be an essential factor for the formation of the “snowflakes.” It may further accelerates the crystal growth along $\langle 100 \rangle$ directions and finally maintains the snowflakelike $\text{WO}_3 \cdot 0.33\text{H}_2\text{O}$ particles. This deduction consists well with our previous research,²⁷ in which the key role of the microwave heating is highlighted to explain the evolution of the complex ZnO morphologies. Likewise, the snowflakelike structure of the orthorhombic $\text{WO}_3 \cdot 0.33\text{H}_2\text{O}$ particles in this research could be attribute to the irradiation of microwave though the specific mechanism of microwave heating needs more research in the future.

In summary, we have successfully synthesized regularly shaped snowflakelike $\text{WO}_3 \cdot 0.33\text{H}_2\text{O}$ particles by using peroxopolytungstic acid under a microwave-assisted hydrothermal condition. It is found that besides the intrinsic crystal nature of the $\text{WO}_3 \cdot 0.33\text{H}_2\text{O}$ particles, microwave heating also plays an important role to form the multilayered snowflakelike microstructures, indicating that the microwave heating may have special influences on the crystal growth of the particles under hydrothermal conditions. Our research provides a facile, template-free approach for the synthesis of hierarchically structured crystal of tungsten oxide hydrates at low temperature with short reaction time. This approach may be applicable in large-scale and green syntheses of various tungsten oxide hydrates and other oxide materials that requiring well-defined shapes and hierarchical structures through facile processes.

The authors are grateful to Research and National Natural Science Foundation of China (No. 50942047) and Innovation Team Assistance Foundation of Shaanxi University of Science and Technology (No. TD09-05).

References

- 1 J. Zhou, Y. Ding, S. Deng, L. Gong, N. Xu, Z. Wang, *Adv. Mater.* **2005**, *17*, 2107.
- 2 P. Li, C. Nan, Z. Wei, J. Lu, Q. Peng, Y. Li, *Chem. Mater.* **2010**, *22*, 4232.
- 3 K. S. Krishna, C. S. S. Sandeep, R. Philip, M. Eswaramoorthy, *ACS Nano* **2010**, *4*, 2681.
- 4 X. Chen, M. Qiao, S. Xie, K. Fan, W. Zhou, H. He, *J. Am. Chem. Soc.* **2007**, *129*, 13305.
- 5 R. Wahab, Y.-S. Kim, K. Lee, H.-S. Shin, *J. Mater. Sci.* **2010**, *45*, 2967.
- 6 K. Kalantar-zadeh, A. Vijayaraghavan, M.-H. Ham, H. Zheng, M. Breedon, M. S. Strano, *Chem. Mater.* **2010**, *22*, 5660.
- 7 S. Yue, L. Zhang, J. Lu, J. Zhang, *Mater. Lett.* **2009**, *63*, 1217.
- 8 Y. Zhang, R. Li, X. Zhou, M. Cai, X. Sun, *Cryst. Growth Des.* **2009**, *9*, 4230.
- 9 T. Thongtem, A. Phuruangrat, S. Thongtem, *J. Mater. Sci.* **2007**, *42*, 9316.
- 10 X. Hu, J. C. Yu, J. Gong, *J. Phys. Chem. C* **2007**, *111*, 11180.
- 11 J. Wang, P. S. Lee, J. Ma, *Cryst. Growth Des.* **2009**, *9*, 2293.
- 12 C.-C. Huang, W. Xing, S.-P. Zhuo, *Scr. Mater.* **2009**, *61*, 985.
- 13 M. Breedon, P. Spizzirri, M. Taylor, J. du Plessis, D. McCulloch, J. Zhu, L. Yu, Z. Hu, C. Rix, W. Wlodarski, K. Kalantar-zadeh, *Cryst. Growth Des.* **2010**, *10*, 430.
- 14 D. Ke, H. Liu, T. Peng, X. Liu, K. Dai, *Mater. Lett.* **2008**, *62*, 447.
- 15 S. Balaji, Y. Djaoued, A.-S. Albert, R. Ferguson, R. Brünig, B.-L. Su, *J. Mater. Sci.* **2009**, *44*, 6608.
- 16 D. Chen, J. Ye, *Adv. Funct. Mater.* **2008**, *18*, 1922.
- 17 S. Jeon, K. Yong, *J. Mater. Chem.* **2010**, *20*, 10146.
- 18 W. Hu, Y. Zhao, Z. Liu, C. W. Dunnill, D. H. Gregory, Y. Zhu, *Chem. Mater.* **2008**, *20*, 5657.
- 19 J. Yu, L. Qi, *J. Hazard. Mater.* **2009**, *169*, 221.
- 20 L. Zhou, J. Zou, M. Yu, P. Lu, J. Wei, Y. Qian, Y. Wang, C. Yu, *Cryst. Growth Des.* **2008**, *8*, 3993.
- 21 J. Wang, P. S. Lee, J. Ma, *J. Cryst. Growth* **2009**, *311*, 316.
- 22 K.-H. Chang, C.-C. Hu, C.-M. Huang, Y.-L. Liu, C.-I Chang, *J. Power Sources* **2011**, *196*, 2387.
- 23 Q. Sun, J. Luo, Z. Xie, J. Wang, X. Su, *Mater. Lett.* **2008**, *62*, 2992.
- 24 S. Yoon, A. Manthiram, *J. Mater. Chem.* **2011**, *21*, 4082.
- 25 M. Godinho, C. Ribeiro, E. Longo, E. R. Leite, *Cryst. Growth Des.* **2008**, *8*, 384.
- 26 M. Siegfried, K.-S. Choi, *Adv. Mater.* **2004**, *16*, 1743.
- 27 J. Huang, C. Xia, L. Cao, X. Zeng, *Mater. Sci. Eng., B* **2008**, *150*, 187.